Published in final edited form as:
Lab Invest. 2013 January ; 93(1): 96–111. doi:10.1038/labinvest.2012.148.

Sonic Hedgehog contributes to gastric mucosal restitution after injury

Chang Xiao[1,*], **Rui Feng**[1,*], **Amy C. Engevik**[1], **Jason R. Martin**[1], **Julie A. Tritschler**[2], **Michael Schumacher**[1], **Robert Koncar**[1], **Joseph Roland**[3], **Ki Taek Nam**[3], **James R. Goldenring**[3,#], and **Yana Zavros**[1]

[1]Department of Molecular and Cellular Physiology, University of Cincinnati, OH

[2]Xavier University, Undergraduate Biology Department, Cincinnati, OH

[3]Nashville VA Medical Center and Departments of Surgery and the Epithelial Biology Center, Vanderbilt University Medical Center, TN

Abstract

Eradication of *Helicobacter pylori* correlates with regeneration of the gastric epithelium, ulcer healing and re-expression of the gastric morphogen Sonic Hedgehog (Shh). We sought to identify the role of Shh as a regulator of gastric epithelial regeneration during wound healing. A mouse model expressing a parietal cell-specific, tamoxifen-inducible deletion of Shh ($HKCre^{ERT2}$;$Shh^{flox/flox}$ or PC-iShhKO) was developed. Stomachs were collected and compared 7 to 150 days after the final vehicle or tamoxifen injection. Ulcers were induced in both controls and PC-iShhKO mice using acetic acid and ulcer size compared 1 and 7 days post induction. 1) *Re-expression of Shh correlates with decreased hyperproliferation:* Compared to controls, PC-iShhKO mice developed foveolar hyperplasia. Restoration of normal gastric epithelial architecture and differentiation correlated with the re-expression of Shh in PC-iShhKO mice 150 days after the final tamoxifen injection. At the tamoxifen dose used to induce Cre recombination there was no genotoxicity reported in either $HKCre^{ERT2}$ or $Shh^{flox/flox}$ control mouse stomachs. 2) *Delayed wound healing in PC-iShhKO mouse stomachs:* To identify the role of Shh in gastric regeneration, an acetic acid ulcer was induced in control and PC-iShhKO mice. Ulcers began to heal in control mice by 7 days after induction. Ulcer healing was documented by decreased ulcer size, angiogenesis, macrophage infiltration and formation of granulation tissue that correlated with the re-expression of Shh within the ulcerated tissue. PC-iShhKO mice did not show evidence of ulcer healing. Re-expression of Shh contributes to gastric regeneration. Our current study may have clinical implications given that eradication of *Helicobacter pylori* correlates with re-expression of Shh, regeneration of the gastric epithelium and ulcer healing.

Keywords

Helicobacter pylori (*H. pylori*); gastric ulcer; re-epithelialization; tissue repair; macrophages

Corresponding Author: Yana Zavros, Ph.D., University of Cincinnati College of Medicine, Department of Molecular and Cellular Physiology, 231 Albert B. Sabin Way, Room 3263 MSB, Cincinnati, OH 45267-0576, Tel: (513) 558-2421, Fax: (513) 558-5738, yana.zavros@uc.edu. #**Contact Dr. JR Goldenring for the $HKCre^{ERT2}$ mice:** James R. Goldenring, M.D., Ph.D., Vanderbilt University Medical Center, Medical Research Building IV, Rm. 10435-G, 2213 Garland Avenue, Nashville, TN 37232, Tel: (615) 936-3726, jim.goldenring@Vanderbilt.edu.
*Authors contributed equally to the preparation of this manuscript

The authors declare no conflict of interest.

Supplementary Information accompanies the paper on the Laboratory Investigation website.

INTRODUCTION

Sonic Hedgehog (Shh) is highly expressed in the adult stomach and functions as a morphogen to drive epithelial cell differentiation (1–3). Earlier studies reported the role of Shh as a gastric morphogen based on evidence that correlated the loss of Shh with inflammation of the adult stomach (4–6). Since then, we have reported that Shh secreted from parietal cells has significant biological activity, regulating the differentiation of cell lineages and controlling gastric physiological function (3). Our previous studies utilized a constitutive HKCre-Shh deficient mouse model of parietal cell-specific Shh loss (3). Thus, in these constitutive HKCre-Shh deficient mice, Shh is deleted during development as soon as the H^+,K^+-ATPase is expressed and is not re-expressed in the gastric parietal cell. In mice, this means Shh would be deleted in parietal cells on embryonic day 19 when H^+,K^+-ATPase initiates expression within parietal cells (7).

The current study uses a refined experimental approach by developing a mouse model expressing a tamoxifen-inducible parietal cell-specific deletion of Shh (PC-iShhKO). There are two major advantages to using the PC-iShhKO mouse model when studying the role of Shh as a regulator of gastric differentiation. The first advantage is that the inducible model gives us the ability to identify the role of Shh signaling in the adult stomach in a fully differentiated epithelium. Second, the PC-iShhKO mice allow the assay of changes in epithelial cell differentiation in relation to the loss and gain of Shh expression, independent of inflammation. Clinically this is important given that re-expression of Shh in *Helicobacter pylori* (*H. pylori*)-infected patients after eradication of bacterial infection promotes regeneration of the gastric epithelium and ulcer healing (5, 6, 8).

Early eradication of *H. pylori* results in re-expression of Shh, with a concomitant restoration of disrupted gastric mucosal architecture (4, 9, 10). Based on such evidence, Shh is implicated in gastric epithelial regeneration (3, 9, 10). However, the role of Shh as a regulator of epithelial differentiation may also be relevant in complex repair mechanisms of the stomach. The gradual increase in Hedgehog signaling at gastric ulcerated margins is accompanied by gland cell proliferation and differentiation, which is blocked by Hedgehog signaling inhibitor cyclopamine (8). Ulcer healing is a complex process that is not completely understood in the stomach, but involves inflammatory cell infiltration, cell proliferation, migration, re-epithelialization and angiogenesis (11). Interestingly, Shh regulates multiple events essential for wound healing in other tissues including the lung (12), bone (13), heart and cornea (14, 15). The immune response is crucial for repair in tissues that include the kidney (16) and skin (17). In particular, macrophages are key immune cells that secrete necessary cytokines, chemokines and pro-angiogenic factors that are necessary regulators for repair (18). Interestingly, Shh is known to act as a monocyte/macrophage chemoattractant during repair of the myocardium (19) and *H. pylori* infection (20). However, whether Shh signaling regulates regeneration of the epithelium by regulating the immune response during tissue repair in the stomach is unclear. Using the PC-iShhKO mouse model, we show that Shh signaling regulates gastric regeneration by inducing inflammatory cell recruitment, neovascularization and re-epithelialization.

MATERIALS AND METHODS

Animals

Mice expressing a tamoxifen-inducible Cre recombinase transgene in gastric parietal cells was developed by cloning the H^+,K^+-ATPase β subunit (parietal cell-specific) promoter (nt −10535-+24; a gift of Dr. Jeffrey Gordon, Washington U., St. Louis) upstream of tamoxifen-inducible Cre-recombinase (Cre^{ERT2}, A gift of Dr. Guoqiang Gu, Vanderbilt University) (21,22). Linearized vector was injected into C57BL/6 mouse oocytes and transgenic mice

were identified and bred in the Vanderbilt Transgenic Mouse Core facility. Mice carrying the transgene were genotyped using PCR of genomic DNA with transgene specific primers (HKATP-Sense: TCACACAGAGGAGACTATAAGCCC and Cre-Antisense: GTGAGATATCTTTAACCCTGATCG). Mice expressing a tamoxifen-inducible parietal cell-specific deletion of Shh ($HKCre^{ERT2}$;$Shh^{flox/flox}$) were developed using transgenic animals bearing loxP sites flanking exon 2 of the Shh gene ($Shh^{flox/flox}$ mice, obtained from Dr. JA Whitsett, Department of Pediatrics, University of Cincinnati Children's Hospital Medical Center with permission from Dr. AP McMahon, Harvard University) crossed with the $HKCre^{ERT2}$ mice. The $Shh^{flox/flox}$ mice were on a 129/Sv background. To achieve inducible deletion of Shh in the stomach, 4-week old $HKCre^{ERT2}$; $Shh^{flox/flox}$ mice were treated with tamoxifen (0.75 mg/day/20g body weight, i.p.) for 5 consecutive days and these mice are designated as the PC-iShhKO group. Mice used as controls included $HKCre^{ERT2}$ and $Shh^{flox/flox}$ animals injected with vehicle (100 μl corn oil, i.p.) or tamoxifen for 5 consecutive days. Mice were then analyzed 7, 60 and 150 days after the final injection.

All mouse studies were approved by the University of Cincinnati Institutional Animal Care and Use Committee (IACUC) that maintains an American Association of Assessment and Accreditation of Laboratory Animal Care (AAALAC) facility.

Gastric acidity

Control and PC-iShhKO mice were injected with either PBS or with 20 mg/kg histamine (i.p.) 30 minutes prior to analysis. Mouse stomachs were opened along the greater curvature and rinsed into 2 ml of normal saline (0.9% NaCl, pH 7.0). Supernatant were collected and titrated with 0.005 N NaOH and gastric acidity was expressed as μEq and values normalized to kg body weight (3).

β-galactosidase (X-gal) staining

To determine the efficiency of recombination, $HKCre^{ERT2}$ mice were crossed with $Rosa26r^{lacZ}$ reporter mice (purchased from The Jackson Laboratory). $HKCre^{ERT2}$ mice were then injected with either vehicle (100 μl corn oil, i.p.) or tamoxifen (0.75 mg/day, i.p.) for 5 days and stomach sections collected. X-gal staining of stomach sections was performed according to the manufacturer's protocol (Sigma Aldrich). Briefly, tissue was fixed in 4% paraformaldehyde/phosphate buffered saline (PBS) before staining with X-gal solution for 24 hours at 37°C in the dark. Sections were rinsed, post-fixed in 10% formalin overnight at 4°C and paraffin embedded.

Immunofluorescence and immunohistochemistry

A longitudinal section of the stomach covering both the fundic and antral regions was fixed in 4% paraformaldehyde/PBS, paraffin-embedded and 3 μm sections were prepared. After deparaffinization, antigen retrieval was performed by heating the slides for 10 minutes at 100°C in 0.01M sodium citrate buffer (Antigen Unmasking Solution, Vector Laboratories, Burlingame, CA). Sections were then blocked using 5% BSA/Tris buffered saline/ 0.1%Tween 80 (TBS-T). To assess the expression of surface mucous pit cells stomach sections were stained with 20 μg/ml *Ulex europaeus* (UEA1) FITC conjugate (Sigma). Sections were also immunostained with a 1:100 dilution of goat anti-Shh (Santa Cruz Biotechnology) followed by a 1-hour incubation with a 1:100 dilution of anti-goat Alexa Fluor 488 secondary antibody (Invitrogen). Tissue was then counterstained with 1 μg H^+,K^+-ATPAse β subunit (Affinity BioReagents) antibody followed by a 1:100 dilution of Alexa Fluor 488 IgG_1 mouse antibody (Invitrogen). All slides were counterstained with nuclear marker anti-TOPRO at a 1:1000 dilution for 20 minutes. For all immunofluorescence staining, coverslips were mounted onto slides with Prolong Gold Antifade Reagent Mounting Medium (Molecular Probes) and analyzed with a Zeiss

LSM510 META confocal microscope. Morphometric analysis was performed by counting 5 well-oriented glands in 5 high power fields (400x, total of 25 glands/section).

For histological evaluation, sections were stained for Hematoxylin and Eosin (H&E). Stomach tissues were fixed in Carnoy's fixative (60% ethanol, 30% chloroform, 10% acetic acid) for 16 hours, paraffin embedded, and 4 μm sections were prepared. After deparaffinization, antigen retrieval was performed by heating the slides for 10 minutes at 100°C in 0.01M sodium citrate buffer (Antigen Unmasking Solution, Vector Laboratories, Burlingame, CA). Endogenous peroxidase activity was then blocked by incubating slides in 3% hydrogen peroxide/ethanol for an additional 20 minutes before incubating for 1 hour with a 1:500 dilution of mouse anti-F4/80 (myeloid cell marker) or 1:200 dilution of rabbit anti-CD31 (Abcam). All slides were incubated with either biotinylated anti-mouse or anti-rabbit secondary antibody for 30 minutes followed by additional 30-minute incubation with ABC reagent (Vectastain ABC kit; Vector Laboratories, Burlingame, CA). Color was developed with 3,3'-diaminobenzidine (DAB) using the DAB Substrate Kit (Vector Laboratories, Burlingame, CA) and slides were then counterstained with hematoxylin (Fisher Scientific Company, Kalamazoo, MI). Positive H+,K+-ATPase (parietal cells)-, CD31- and F4/80-cells were counted in 10 random high power fields 400x.

Experimental Gastric Ulcer Induction

Four-week old $HKCre^{ERT2}$ or $Shh^{flox/flox}$ mice were injected with vehicle or tamoxifen (control group) and $HKCre^{ERT2}$; $Shh^{flox/flox}$ mice were injected with tamoxifen (PC-iShhKO group) as described in the *Animals* section and 14 days after the final injection ulcers were induced as previously described (23). Mice were anaesthetized using isoflurane and a midline abdominal laparotomy was then performed to expose the stomach. Glacial acetic acid (100%) or sterile PBS was applied to the serosal surface for 25 seconds using a capillary tube with a 0.5 mm diameter. The abdominal incision was sutured in 2 layers and mice were analyzed 1, 2, 3, 4, 5 and 7 days after surgery.

Laser Capture Microdissection (LCM)

Laser capture microdissection (LCM) was used to determine the expression pattern of Shh, Ihh, MUC5AC, Atp4α, MUC6, pepsinogen (PgC), Ang1 and VEGF in the gastric epithelium. Slide-mounted 8 μm frozen sections were stained using the HistoGene LCM Frozen Section Staining Kit (Molecular Devices, Sunnyvale, CA) and dehydrated (30 second ethanol submersions followed by a 5 minute submersion in xylene and a 5 minute drying period). Cells specific to each region were isolated using the Molecular Devices/ Arcturus VERITAS Laser-Capture Microdissection System (Model 704, California). First the UV cutting laser (laser power 10–15% of total laser output) was used to ablate the cells surrounding either the surface pit region or mucous neck cells surrounding the parietal cells within the neck region. An infrared laser power of 70 mW and pulse of 250 μsec was then used to capture the cells.

Quantitative RT-PCR (qRT-PCR)

Total RNA was isolated from LCM tissue collected from both Control and PC-iShhKO mice using the Arcturus PicoPure RNA Isolation Kit (Molecular Devices) and from flow sorted cells using an RNeasy Mini Kit (Qiagen, Cat. 74104). The High Capacity cDNA Reverse Transcription Kit (Applied Biosystems) was used for cDNA synthesis of RNA following the recommended protocol. For each sample 60 ng of RNA was reverse transcribed to yield approximately 2 μg total cDNA that was then used for the real-time PCR. Predesigned Real-Time PCR assays were purchased for the following genes (Applied Biosystems): Shh (Mm00436528_m1), HPRT (Mm00446968_m1), Ang1 (Mm00456503_m1), VEGF (Mm01281449_m1), MUC5AC (Mm01276711_mh), Atp4a (Mm01176574_g1), MUC6

(Mm00725185_g1), Gli1 (Mm00494654_m1), and Hhip (Mm00469580_m1). PCR amplifications were performed in a total volume of 20 μl, containing 20X TaqMan Expression Assay primers, 2X TaqMan Universal Master Mix (Applied Biosystems, TaqMan® Gene Expression Systems) and cDNA template. Each PCR amplification was performed in duplicate wells in a StepOne™ Real-Time PCR System (Applied Biosystems), using the following conditions: 50°C 2 minutes, 95°C 10 minutes, 95°C 15 seconds (denature) and 60°C 1 minute (anneal/extend) for 40 cycles. Fold change was calculated as: $(C_t\text{-}C_{t\ high}) = n_{\ target}$, $2^{ntarget}/2^{nHPRT}$ = fold change where C_t = threshold cycle. The results were expressed as average fold change in gene expression relative to control with HPRT used as an internal control according to Livak and Schmittgen (24).

Enzyme-Linked Immunosorbent Assay (ELISA)

Tissue was homogenized in phosphate buffered saline supplemented with protease inhibitor (Roche) and centrifuged for 30 minutes at 13,000rpm at 4°C. Cytokine MIP-1α and VEGF concentrations in the tissue sample supernatants and plasma Shh levels were determined by enzyme-linked immunosorbent assay (ELISA) (Millipore, Billerica, MA) according to manufacturer's protocol. Concentrations were calculated from standard curves using recombinant proteins and expressed in pg/ml. The cytokine analysis was performed by the Cytokine and Mediator Measurement Core laboratory (Cincinnati Children's, Digestive Health Center).

Western blot

Tissue was homogenized in 0.5 ml protein lysis buffer (300 mM NaCl, 30 mM Tris, 2 mM $MgCl_2$, 2 mM CaCl2, 0.1% Triton-X100, pH 7.4), centrifuged at 15,000 g for 10 minutes and supernatant collected. Tissue protein extracts (50 μg total protein) were loaded on a 4–20% sodium dodecyl sulfate-polyacrylamide gradient gel (Invitrogen). Proteins were transferred to membranes (Hybond-C Extra Nitrocellulose, Fisher Scientific) that were then blocked with Detector Block (KPL) for 1 h at room temperature. Membranes were then incubated with a 1:100 dilution of goat anti-Shh (N-19, sc-1194, Santa Cruz Biotechnology) and 1:2000 dilution of mouse anti-glyceraldehyde 3-phosphate dehydrogenase (GAPDH) (CHEMICON, Temecula, CA). Membranes were then incubated for 1 hour at room temperature with a 1:1000 dilution of Alexa Fluor 680 anti-goat, anti-rabbit antibody or anti-mouse antibodies (Invitrogen/ Molecular Probes). Proteins were visualized and quantified using the Odyssey Infrared Imaging System software.

Flow Cytometry and Fluorescence-activated cell sorting (FACS)

Gastric epithelial cells were enzymatically dissociated and collected according to a previously published protocol (25). Briefly, whole stomach was collected, opened along the greater curvature, washed in PBS and cut into 2 mm^2 pieces. Tissue was digested in RPMI 1640 supplemented with 1mM DTT and 1mM EDTA for 1 hour at 37°C while shaking. Cells were collected by passing supernatant through a 40 μm cell strainer. Tissue was further digested using RPMI 1640 supplemented with 5% BSA and 1.5mg/ml Dispase II (Roche) for 1.5 hours at 37°C while shaking. Cells were collected by passing supernatant through 40μm cell strainer and pooling with cells from first digest. Cells collected from the gastric digest and blood were resuspended in PBS with 5% BSA, and incubated with CD16/CD32 FcBlock (BD Biosciences, Cat. 553141) for 5 minutes at 4°C. Next, cells were labeled using a 1:100 concentration of APC-conjugated F4/80 (Invitrogen, MF48005) and FITC-conjugated CD11b (Invitrogen, RM2801) for 20 minutes at room temperature and then fixed with fixative medium A (Invitrogen) for 15 minutes at room temperature. Cells used for flow sorting were not fixed. Unstained and single-stained cells, and FMO (fluorescence minus one) controls were used as compensation controls. Cells were resuspended in 500 μl PBS containing 5% BSA and analyzed on a FACSCalibur flow cytometer (BD Biosciences)

or re-suspended in basic sorting buffer (PBS, 0.5% fetal bovine serum, 1 mmol/L EDTA) for sorting using a FACSAria II cell sorter (BD Biosciences). For sorting, cells were gated for F480+ and collected in lysis buffer for RNA extraction. Analysis was performed using FlowJo software (Tree Star, Ashland, OR).

Statistical analysis

The significance of the results was tested by a one-way ANOVA, two-way ANOVA or unpaired t-test using commercially available software (GraphPad Prism, GraphPad Software, San Diego, CA). A P value <0.05 was considered significant.

RESULTS

A mouse model expressing a tamoxifen-inducible and parietal cell-specific Shh deletion (PC-iShhKO)

To assess the role of Shh as a regulator of gastric epithelial cell differentiation and tissue repair, a mouse model expressing a parietal cell-specific deletion of Shh ($HKCre^{ERT2}$; $Shh^{flox/flox}$) was developed. $HKCre^{ERT2}$ mice were developed using the 1.3 kb alpha-H/K-ATPase promoter previously described by Gordon and colleagues (22) to drive parietal cell expression of tamoxifen-inducible Cre recombinase (Cre^{ERT2}). The targeting of Cre recombinase expression was first determined by crossing the $HKCre^{ERT2}$ mice with the $Rosa26R^{lacZ}$ reporter mice. $HKCre^{ERT2}$ mice were then injected with either vehicle or tamoxifen followed by X-gal staining of stomach sections. Stomachs that were collected from tamoxifen-treated $Rosa26R^{lacZ}$ reporter mice crossed with $HKCre^{ERT2}$ animals exhibited β-galactosidase activity in parietal cells in the corpus region of the stomach (Figure 1A, B). β-galactosidase activity was not observed in the antrums of $HKCre^{ERT2}$ animals treated with tamoxifen (Figure 1C). No β-galactosidase activity was detected in the sections collected from the $Rosa26R^{lacZ}$ reporter mice crossed with $HKCre^{ERT2}$ animals treated with vehicle (Figure 1D).

Deletion of Shh within the parietal cells was confirmed at the gene level by laser capture microdissection (LCM). Cells from the neck and pit region of the stomach were sampled from control mouse stomachs. The expression of 3 marker genes: ATP4α (parietal cells), MUC5AC (surface pit cells) and MUC6 (neck cells) were determined by qRT-PCR. Relative to the pit epithelium, the expression of ATP4α (parietal cells marker) and MUC6 (a mucous neck cell marker) were higher in RNA collected from the neck region, while expression of MUC5AC (a surface mucous cell marker) was lower in the neck region (Figure 1E). Cells were also collected from the neck and pit region of control and PC-iShhKO mouse stomachs 7 days after the final vehicle or tamoxifen injection (Figure 1F). Compared to the control group where Shh mRNA expression was detected in the neck region of the stomach, Shh expression was significantly decreased in the same region collected from PC-iShhKO mice (Figure 1F). Although Ihh expression was detected in both the pit and neck regions of control and PC-iShhKO mouse stomachs, Ihh expression was significantly greater in PC-iShhKO mice relative to controls (Figure 1F). The increased Ihh expression measured in the PC-iShhKO mice correlated with an increase in Gli1 expression in the pit region that was indicative of the activation of the Hedgehog signaling pathway (Figure 1F).

It has been reported that the inducible Cre recombinase system to delete genes using high doses of tamoxifen leads to the development of spasmolytic polypeptide-expressing metaplasia in the stomach, atrophy of the entire epithelium and hyperplasia by 2 weeks even in the absence of loxP-flanked alleles (26). Thus, it was important to determine the Cre-induced genotoxicity with the tamoxifen dose used in the current study. Both $HKCre^{ERT2}$

and $Shh^{flox/flox}$ mice were injected with either vehicle (100 μl corn oil, i.p.) or tamoxifen (0.75 mg/day/20g body weight, i.p.) for 5 consecutive days and stomach analyzed 7 and 30 days after the final injection by histology. H&E staining shown in Supplemental Figure 1A–H demonstrate that, at the tamoxifen dose used to induce Cre recombination in the $HKCre^{ERT2}$;$Shh^{flox/flox}$ mice, there was no genotoxicity reported in either the $HKCre^{ERT2}$ or $Shh^{flox/flox}$ mice. Therefore, at a tamoxifen dose of 0.75 mg/day/20g body weight Cre recombination did not have a genotoxicity effect, and this was consistent with published data using a similar dose (26,27).

Re-expression of Shh in the gastric epithelium correlates with decreased hyperproliferation of the surface mucous pit cell lineage

Histological analysis using H&E stained paraffin gastric sections showed a number of changes within the epithelium of PC-iShhKO mice that were consistent with the mouse model expressing a constitutively deleted gastric Shh deletion (HKCre; $Shh^{flox/flox}$) previously reported (3). Histological evaluation of PC-iShhKO mouse stomach 7 days post-tamoxifen injection showed areas of expanded surface mucous cells (foveolar hyperplasia) in the fundic epithelium (Figure 2B) compared to the normal gastric mucosa of vehicle controls (Figure 2A). Expansion of the surface mucous cells and cystic glands were apparent 60 days after the final tamoxifen injection in the stomachs of PC-iShhKO mice (Figure 2D) compared to the normal gastric histology in control mice (Figure 2C). Importantly, the histology of PC-iShhKO mouse stomachs 150 days post-tamoxifen injection was normal lacking either expansion of the surface mucous cells or cystic glands (Figure 2F) and was similar to the vehicle-injected control group (Figure 2E).

Re-expression of Shh within the gastric epithelium was corroborated at the gene level by laser capture microdissection (LCM). Cells from the neck region of the stomach were sampled from control and $HKCre^{ERT2}$;$Shh^{flox/flox}$ (PC-iShhKO) mouse stomachs. Compared to the control group where Shh mRNA expression was detected in the neck region of the stomach, Shh expression was significantly decreased in the same region collected from PC-iShhKO mice 7 days after tamoxifen injection (Figure 3A), verifying the successful deletion of Shh. PC-iShhKO mice analyzed 60 days after the final tamoxifen-injection showed increased Shh expression compared to the 7 day tamoxifen-treated $HKCre^{ERT2}$;$Shh^{flox/flox}$ mice, but significantly lower than the control group (Figure 3B). Compared to the control group, 5 months after the final tamoxifen injection, PC-iShhKO mice showed re-expression of Shh expression (Figure 3C).

Total parietal cell number remained unchanged in the PC-iShhKO mouse stomachs when compared to cell numbers in the controls (Supplemental Figure 2). Although there was a clear deletion of Shh within the parietal cells of the PC-iShhKO mice (Supplemental Figure 2B) compared to controls (Supplemental Figure 2A), total parietal cell number remained similar to cell numbers quantified in control mouse stomachs (Figure 2C). However, parietal cell function was lost in the PC-iShhKO (Supplemental Figure 2D). PC-iShhKO mouse parietal cells did not secrete acid in response to histamine stimulation (Supplemental Figure 2D). These findings were similar with our previous report that in the HKCre/Shh^{KO} mouse stomach parietal cell number was unchanged (3).

Changes in the surface mucous cells were quantified by immunofluorescence staining using lectin *Ulex europaeus I (UEAI)*. An expansion in the surface mucous cells was observed in the stomachs of PC-iShhKO mice compared to controls 7 (Figure 4A) and 60 (Figure 4B) days after the final tamoxifen injection. By 150 days after injection, surface mucous cell numbers were comparable between control and PC-iShhKO mice (Figure 4C). Morphometry confirmed the expansion of the surface mucous cells in the PC-iShhKO mouse stomachs 7 (Figure 4D) and 60 (Figure 4E) days post-tamoxifen injection, foveolar hyperplasia was not

observed at 150 days after treatment (Figure 4F). Interestingly, normalization of the gastric lineages in PC-iShhKO mice was consistent with the approximate parietal cell turnover rate of 164 days (28).

Deletion of Shh also correlated with an increase in Ki67 positive nuclei in the gastric mucosa of tamoxifen-treated $HKCre^{ERT2};Shh^{flox/flox}$ mice (PC-iShhKO) compared to controls at 7 (Figure 4G) and 60 (Figure 4H) days after injection. Re-expression of Shh in the parietal cells of PC-iShhKO mice resulted in a reduction in proliferation to levels equivalent to those observed in the control animals and normalization of the gastric epithelial morphology (Figure 4I).

Collectively, data from the PC-iShhKO mouse model extends our previous findings(3) by demonstrating that re-expression of Shh correlates with restoration of the normal gastric epithelial morphology.

PC-iShhKO mice exhibit delayed wound healing in response to acetic acid injury

To identify the role of Shh as a regulator of gastric wound repair, ulcers in the fundic region of control and PC-iShhKO mice were induced using an established acetic acid ulceration model (23). Stomachs were examined 1 to 7 days after ulcer induction. Figures 5A and C show representative photographs of gastric ulcers from control and PC-iShhKO mice. Ulcer size significantly decreased in control mice (Figure 5B) compared to PC-iShhKO animals (Figure 5D) 7 days after ulcer induction.

Stomach sections were then examined for changes in histology (Figure 5E, F). On day 1 after ulcer induction, control mice exhibited lesions with distinct margins formed around the ulcer (data not shown). Seven days after ulcer induction, control mice exhibited granulation tissue below the ulcer (Figure 5E). The appearance of epithelial cells at the base of the ulcer margin invading the granulation tissue was observed in the control mice (Figure 5E), but absent in the PC-iShhKO group (Figure 5F). PBS controls for control and PC-iShhKO mice are shown in Supplemental Figure 2A–D. Collectively, these data demonstrate that loss of Shh in parietal cells results in delayed wound healing in response to gastric injury.

Shh protein is re-expressed in the ulcerated tissue within 2 days post-injury

To quantify the re-expression of Shh protein during repair, stomach tissue was collected from the ulcerated area from control and PC-iShhKO mice 1 to 7 days post-injury. Western blot analysis showed a loss of Shh protein expression within 24 hours post-injury in controls (Figure 6A). At day 2 there was a significant increase in Shh expression that continued to increase over the next 7 days (Figure 6, B). Shh protein expression was undetected in the injured tissue of PC-iShhKO mouse stomachs (Figure 6A). Figure 6C shows the concentrations of circulating Shh measured by ELISA using plasma collected from both controls and PC-iShhKO mice 3 days post-injury. In plasma collected from controls, there was a significant increase in circulating Shh concentrations in response to acetic acid-induced gastric injury. Changes in circulating Shh concentrations were not observed in plasma collected from PC-iShhKO in response to a similar injury. In addition, immunofluorescence staining using an anti-Shh antibody revealed that within the ulcerated margin of the control epithelium there was strong re-expression of Shh 3 days post-injury that is not observed in the stomachs of the PC-iShhKO group (Figures 6D and F). Immunostaining for Shh within the injured tissue showed that there was also an infiltration of Shh-expressing cells within the granulation tissue (Figure 6D and E, **indicated by arrows**). However, the identity of these cells is yet to be determined. To address the question of the timing of repair a co-immunofluorescene stain was performed using parietal cell specific and anti-Shh specific antibodies. Re-expression of Shh was observed at the

ulcerated margins and within the granulation tissue within the injured tissue 3 days post-surgery. Very few parietal cells were detected within the injured tissue thus is unlikely that re-expression of Shh is a consequence of parietal cell recovery (Figure 6G).

Collectively these data demonstrate that Shh is expressed and secreted from the gastric epithelium within 3 days of gastric injury and thus supports a critical role for Hedgehog signaling in the initiation of the repair mechanism. However, it is important to consider that re-expression of Shh within the injured gastric tissue is also attributed to the infiltration of Shh-expressing cells that may provide additional regulatory mechanisms for repair.

Increase in monocytic cell infiltration and pro-angiogenic factors are lost in PC-iShhKO mice

Macrophages are typically recruited to the ulcer site and are known to secrete crucial growth factors and cytokines necessary for wound repair (11). Indeed, we observed an increase in the myeloid cell number at the ulcer site of control mice 1 day after induction (Figure 7A, B). By marked contrast to the control group, PC-iShhKO mice did not show recruitment of macrophages 2 days after ulcer induction (Figure 7C, D). Quantification of macrophage cell numbers by flow cytometry revealed a significant increase in infiltrating F4/80+CD11b+ cells in the stomachs of injured controls within 2 days (Figure 7E) but absent in the PC-iShhKO group (Figure 7E). In vivo, MIP-1α is among the factors produced by macrophages that induce the local inflammatory response. Consistent with the infiltration of macrophages within control stomachs was a significant increase in the MIP-1α tissue concentrations (Figure 7F), not observed in the PC-iShhKO mice (Figure 7F) in response to injury.

To identify the role of Shh as a chemoattractant for macrophages, activation of Hedgehog signaling was measured by qRT-PCR (Gli1 and Hhip) in cells sorted by fluorescence-activated cell sorting (FACS) from blood and tissue collected from PBS- and acetic acid-induced control and PC-iShhKO mice (Figure 8). Based on the F4/80+ gating shown in the representative flow cytometric contour plots in Figure 8 macrophages were sorted from both blood (Figure 8A, B) and gastric ulcerated tissue (Figure 8C, D). Gli1 and Hhip expression was analyzed by qRT-PCR. While there was no expression of Gli1 and Hhip detected in macrophages isolated from blood and tissue of the PBS-induced group, there was a significant induction in both Hedgehog target genes in the acetic acid-induced mice (Figure 8B, D, E). Activation of Gli1 and Hhip was not observed in the PC-iShhKO groups (Figure 8E).

Taking into consideration that angiogenesis is another essential process for the restoration of the microvasculature within the ulcer (11), expression of pro-angiogenic factors Ang1 and VEGF were quantified. Immunostaining of the stomachs collected from control mice 7 days after acetic acid injury showed an increase in CD31 positive microvessels compared to the PBS treated group (Figure 9A, B and E). Interestingly, PBS-treated PC-iShhKO mice had significantly decreased CD31 positive microvessels compared to the control group and these numbers did not significantly change even with acetic acid injury (Figure 9C, D, E). Expression of pro-angiogenic factor VEGF was quantified within tissue collected from the granulation tissue within the ulcerated region. Compared to the controls, PC-iShhKO mice did not exhibit an increase in VEGF tissue concentrations 2 days after ulcer induction (Figure 9F). Collectively these data demonstrate that loss of Shh results in disrupted regeneration of the gastric epithelium in response to injury. Shh may promote re-epithelialization of the gastric epithelium during wound healing by inducing the restoration of the microvasculature within the injured area.

DISCUSSION

The PC-iShhKO mice have given us the ability to identify the role of Shh signaling in the adult stomach in a fully differentiated epithelium, in relation to the loss and gain of Shh expression. Morphological changes within the stomach in response to Shh deletion were rapid in the inducible PC-iShhKO mice compared to what was reported in the HKCre/Shh^{KO} mice (3). Significant changes in differentiation, histology and function were not observed until after 2 months of age in the HKCre/Shh^{KO} constitutive knockout mice (3) compared to within 7 days in the PC-iShhKO animals where the gastric epithelium was fully differentiated before deletion of Shh. Normalization of the gastric lineages in PC-iShhKO mice was consistent with the approximate parietal cell turnover rate of 164 days (28). The inconsistency in the timing of emergence of this phenotype suggests that deletion of Shh from parietal cells does not affect the developmental patterning of the gastric epithelium, but impairs the epithelial cell differentiation in the fully developed adult stomach.

Studies have correlated Shh re-expression with restoration of gastric mucosal architecture after *H. pylori* eradication (9, 10, 29). However, since the application of antibiotics also causes cessation of inflammation, the direct contribution of Shh on gastric epithelial normalization is unclear from such studies. In the PC-iShhKO mouse model, the gastric epithelium was fully differentiated before Shh was deleted. Re-expression of Shh may have occurred from new parietal cells differentiated from non-targeted progenitor cells. Thus, both the loss and the gain of Shh expression during the clinical process of *H. pylori* infection and eradication was recapitulated in the PC-iShhKO mouse model independent of inflammation. Collectively, the studies identified that Shh is a critical morphogen in the adult stomach that drives epithelial cell differentiation.

Tissue repair in the PC-iShhKO mice was disrupted, as documented by unchanged ulcer size and the lack of re-epithelialization within the wound. This finding was consistent with the study from Kang *et al.* (8) demonstrating that mice treated with the Hedgehog signaling inhibitor cyclopamine blocked cell differentiation at the ulcer margins. Our study advances these findings by using a mouse model that allows us to specifically delete Shh from the parietal cells in the fully differentiated stomach prior to injury.

We observed that compared to the controls, PC-iShhKO mice have delayed gastric repair in response to acetic acid-induced gastric injury. There are two plausible mechanisms that could explain our observations. The first is that injury induces the immune response, including macrophage recruitment, subsequently leading to re-epithelialization and neovascularization. In this first mechanism re-epithelialization may explain the re-expression of Shh within newly formed glands. However, this would not explain the lack of macrophage recruitment and disrupted repair that was observed in the PC-iShhKO mice. Therefore, a second mechanism is one whereby injury results in the induction of Shh expression from the surrounding epithelium and infiltrating Shh-expressing cells (as observed in Figure 6) that subsequently recruits macrophages to the site of injury and thus triggering repair. The second mechanism suggests that deleting Shh from this pathway, as we have done using the PC-iShhKO mice, would result in disruption of macrophage recruitment and subsequent repair.

The PC-iShhKO mice also had decreased macrophage cell infiltration and neovascularization. These findings suggest plausible mechanisms by which Shh promotes tissue repair in the adult stomach. Macrophages are highly versatile cells that are capable of switching phenotypes and cytokine secretion profiles during different phases of tissue repair. During skeletal muscle regeneration, macrophages are first recruited as phagocytic cells with elevated release of pro-inflammatory cytokines such as interleukin 1β (IL-1 β) and

tumor necrosis factor α (TNF-α), and then rapidly convert into an anti-inflammatory phenotype to promote myogenesis (30). Moreover, during regeneration in the injured kidney, macrophages produce Wnt7b that stimulate tissue repair (16). Shh modulates cytokine expression from macrophages (31) and acts as a monocyte chemoattractant (19). Thus, we may speculate that disrupted wound healing observed in the PC-iShhKO mice be explained by insufficient macrophage recruitment and differentiation. A recent study by our group using bone marrow chimera experiments with donor cells collected from mice that have a myeloid cell-specific deletion of the Hedgehog signal transduction protein smoothened (*LysMCre/Smo*^{KO}), demonstrates that Shh signals to the macrophages to induce recruitment during the initiation of gastritis in response to *H. pylori* (20). Whether a similar mechanism exists during the repair of gastric tissue in response to injury remains to be determined.

The PC-iShhKO mice also had decreased neovascularization in response to gastric injury. This finding was documented by decreased expression of pro-angiogenic factor VEGF in the ulcerated granulation tissue in the PC-iShhKO mice compared the controls. In support of our findings, treatment of Shh-encoding plasmid at the site of myocardial ischemia in mice induces the expression of pro-angiogenic factors such as VEGF and Ang-1, and increases the density of both capillaries and arterioles in the injured area (14). In rats, treatment of exogenous Shh results in vessel-like tube formation in injured corneas, which is counteracted by cyclopamine treatment (15). Injection of rmShh at the site of gastric injury also induces a striking increase in both VEGF and Ang1 (Xiao and Zavros, unpublished data). However, to our knowledge this is the first report documenting a role of Shh signaling in neovascularization in the stomach during repair. Thus, further investigation is warranted to identify the exact mechanism of Shh effects during gastric epithelial cell regeneration and wound healing. Clinically this is important given that re-expression of Shh in *H. pylori*-infected patients after eradication of bacterial infection results in the regeneration of the gastric epithelium and ulcer healing (5, 6, 8).

Supplementary Material

Refer to Web version on PubMed Central for supplementary material.

Acknowledgments

This work was supported by NIH 1R01DK083402 grant (Y. Zavros). Work was also supported in part by the Digestive Health Center Cincinnati Children's Medical Health Center (DHC: Bench to Bedside Research in Pediatric Digestive Disease) CHTF/SUB DK078392. These studies were supported by grants to J.R.G. from a Department of Veterans Affairs Merit Review Award, NIH RO1 DK071590, and the AGA Funderburg Award in Gastric Biology Related to Cancer. Transgenic Mouse development utilized the facilities of the Vanderbilt Transgenic Mouse Core Facility supported by the Vanderbilt Digestive Disease Research Center (P30 DK58404) and the Vanderbilt-Ingram Cancer Center (CA68485). We would like to acknowledge the assistance of Monica DeLay manager of the Research Flow Cytometry Core in the Division of Rheumatology at Cincinnati Children's Hospital Medical Center, supported in part by NIH AR-47363. All flow cytometric data were acquired using equipment maintained by the Research Flow Cytometry Core in the Division of Rheumatology at Cincinnati Children's Hospital Medical Center, supported in part by NIH AR-47363. We also acknowledge the assistance of Dr. Marsah Wils-Karp and Alyssa Sproles of The Cincinnati Cytokine/Chemokine/Mediator Measurement Core at the Digestive Health Center Cincinnati Children's Medical Health Center.

Abbreviations

Shh	Sonic Hedgehog
Ptch 1	Patched receptor 1
Smo	Smoothened

Gli1	Glioma-associated Oncogene homolog 1
Ang1	Angiopoietin 1
VEGF	vascular endothelial growth factor
PC-iShhKO	tamoxifen-inducible parietal cell-specific Shh deletion
Hhip	Hedgehog Interacting Protein

REFERENCES

1. Zavros Y, Orr MA, Xiao C, Malinowska DH. Sonic hedgehog is associated with H+,K+-ATPase-containing membranes in gastric parietal cells and secreted with histamine stimulation. Am J Physiol. 2008; 295:G99–G111.
2. Waghray M, Zavros Y, Saqui-Salces M, El-Zaatari M, Alamelumangapuram CB, Todisco A, et al. Interleukin-1beta Promotes Gastric Atrophy Through Suppression of Sonic Hedgehog. Gastroenterology. 2010; 138:562–572. [PubMed: 19883649]
3. Xiao C, Ogle SA, Schumacher MA, Orr-Asman MA, Miller ML, Lertkowit N, et al. Loss of Parietal Cell Expression of Sonic Hedgehog Induces Hypergastrinemia and Hyperproliferation of Surface Mucous Cells. Gastroenterology. 2010; 138(2):550–561. [PubMed: 19909751]
4. van den Brink GR, Hardwick JC, Nielsen C, Xu C, ten Kate FJ, Glickman J, et al. Sonic hedgehog expression correlates with fundic gland differentiation in the adult gastrointestinal tract. Gut. 2002; 51(5):628–633. [PubMed: 12377798]
5. Shiotani A, Iishi H, Uedo N, Ishiguro S, Tatsuta M, Nakae Y, et al. Evidence that loss of sonic hedgehog is an indicator of Helicobacter pylori-induced atrophic gastritis progressing to gastric cancer. Am J Gastroenterol. 2005; 100(3):581–587. [PubMed: 15743355]
6. Suzuki H, Minegishi Y, Nomoto Y, Ota T, Masaoka T, van den Brink GR, et al. Down-regulation of a morphogen (sonic hedgehog) gradient in the gastric epithelium of Helicobacter pylori-infected Mongolian gerbils. J Pathol. 2005; 206(2):186–197. [PubMed: 15818572]
7. Pettitt JM, Toh B, Callaghan JM, Gleeson PA, Van Driel IR. Gastric parietal cell development: Expression of the H+/K+ ATPase subunits coincides with the biogenesis of the secretory membranes. Immunology and Cell Biology. 1992; 71(3):191–200. [PubMed: 8394281]
8. Kang DH, Han ME, Song MH, Lee YS, Kim EH, Kim HJ, et al. The role of hedgehog signaling during gastric regeneration. J Gastroenterol. 2009; 44(5):372–379. [PubMed: 19291354]
9. Nishizawa TSH, Masaoka T, Minegishi Y, Iwasahi E, Hibi T. Helicobacter pylori eradication restored sonic hedgehog expression in the stomach. Hepatogastroenterology. 2007; 54(75):697–700. [PubMed: 17591044]
10. Nishizawa TSH, Nakagawa I, Minegishi Y, Masaoka T, Iwasaki E, Hibi T. Early Helicobacter pylori Eradication Restores Sonic Hedgehog Expression in the Gastric Mucosa of Mongolian Gerbils. Digestion. 2009; 79(2):99–108. [PubMed: 19295210]
11. Tarnawski AS. Cellular and molecular mechanisms of gastrointestinal ulcer healing. Dig Dis Sci. 2005; 50(Suppl 1):S24–S33. [PubMed: 16184417]
12. Fitch PM, Howie SE, Wallace WA. Oxidative damage and TGF-β differentially induce lung epithelial cell sonic hedgehog and tenascin-C expression: implications for the regulation of lung remodelling in idiopathic interstitial lung disease. Int J Exp Pathol. Feb; 2011 92(1):8–17. [PubMed: 21039988]
13. Levi B, James AW, Nelson ER, Li S, Peng M, Commons GW, Lee M, Wu B, Longaker MT. Human adipose-derived stromal cells stimulate autogenous skeletal repair via paracrine Hedgehog signaling with calvarial osteoblasts. Stem Cells Dev. Feb; 2011 20(2):243–257. [PubMed: 20698749]
14. Palladino M, Gatto I, Neri V, Straino S, Silver M, Tritarelli A, et al. Pleiotropic beneficial effects of sonic hedgehog gene therapy in an experimental model of peripheral limb ischemia. Mol Ther. 2011; 19(4):658–666. [PubMed: 21224834]

15. Fujita K, Miyamoto T, Saika S. Sonic hedgehog: its expression in a healing cornea and its role in neovascularization. Mol Vis. 2009; 15:1036–1044. [PubMed: 19471603]
16. Lin SL, Li B, Rao S, Yeo EJ, Hudson TE, Nowlin BT, et al. Macrophage Wnt7b is critical for kidney repair and regeneration. Proc Natl Acad Sci U S A. 2010; 107(9):4194–4199. [PubMed: 20160075]
17. Mahdavian Delavary B, van der Veer WM, van Egmond M, Niessen FB, Beelen RH. Macrophages in skin injury and repair. Immunobiology. Jul; 2011 216(7):753–62. [PubMed: 21281986]
18. Ricardo SD, van Goor H, Eddy AA. Macrophage diversity in renal injury and repair. J Clin Invest. Nov; 2008 118(11):3522–3530. [PubMed: 18982158]
19. Dunaeva M, Voo S, van Oosterhoud C, Waltenberger J. Sonic hedgehog is a potent chemoattractant for human monocytes: diabetes mellitus inhibits Sonic hedgehog-induced monocyte chemotaxis. Basic Res Cardiol. 2010; 105(1):61–71. [PubMed: 19629560]
20. Schumacher MA, Donnelly JM, Engevik AC, Xiao C, Yang L, Kenny S, et al. Gastric Sonic Hedgehog Acts as a Macrophage Chemoattractant During the Immune Response to Helicobacter pylori. Gastroenterology. May; 2012 142(5):1150–1159. e6. [PubMed: 22285806]
21. Means AL, Xu Y, Zhao A, Ray KC, Gu G. A CK19(CreERT) knocking mouse line allows for conditional DNA recombination in epithelial cells in multiple endodermal organs. Genesis. 2008; 46(6):318–323. [PubMed: 18543299]
22. Li Q, Karam SM, Gordon JI. Diphtheria toxin-mediated ablation of parietal cells in the stomach of transgenic mice. J Biol Chem. 1996; 271(7):3671–3676. [PubMed: 8631979]
23. Okabe S, Amagase K. An overview of acetic acid ulcer models--the history and state of the art of peptic ulcer research. Biol Pharm Bull. 2005; 28(8):1321–1341. [PubMed: 16079471]
24. Livak K, Schmittgen T. Analysis of relative gene expression data using real-time quantitative PCR and the 2(−Delta Delta C(T)) Method. Methods. 2001; 25(4):402–408. [PubMed: 11846609]
25. Zavros Y, Rieder G, Ferguson A, Samuelson LC, Merchant JL. Genetic or chemical hypochlorhydria is associated with inflammation that modulates parietal and G-cell populations in mice. Gastroenterology. 2002; 122(1):119–133. [PubMed: 11781287]
26. Jae Huh W, Mysorekar IU, Mills JC. Inducible activation of Cre recombinase in adult mice causes gastric epithelial atrophy, metaplasia, and regenerative changes in the absence of "floxed" alleles. Am J Gastroenterol. 2010; 299(2):G368–G380.
27. Huh WJ, Esen E, Geahlen JH, Bredemeyer AJ, Lee AH, Shi G, et al. XBP1 Controls Maturation of Gastric Zymogenic Cells by Induction of MIST1 and Expansion of the Rough Endoplasmic Reticulum. Gastroenterology. 2010 In Press.
28. Li H, Helander HF. Parietal cell kinetics after administration of omeprazole and ranitidine in the rat. Scand J Gastroenterol. 1995; 30(3):205–209. [PubMed: 7770707]
29. Cai XCJ, Stoicov C, Li H, Wang TC, Houghton J. Helicobacter felis eradication restores normal architecture and inhibits gastric cancer progression in C57BL/6 mice. Gastroenterology. 2005; 128:1937–1952. [PubMed: 15940628]
30. Arnold L, Henry A, Poron F, Baba-Amer Y, van Rooijen N, Plonquet A, et al. Inflammatory monocytes recruited after skeletal muscle injury switch into antiinflammatory macrophages to support myogenesis. J Exp Med. 2007; 204(5):1057–1069. [PubMed: 17485518]
31. Wakelin SJ, Forsythe JL, Garden OJ, Howie SE. Commercially available recombinant sonic hedgehog up-regulates Ptc and modulates the cytokine and chemokine expression of human macrophages: an effect mediated by endotoxin contamination? Immunobiology. 2008; 213(1):25–38. [PubMed: 18207025]

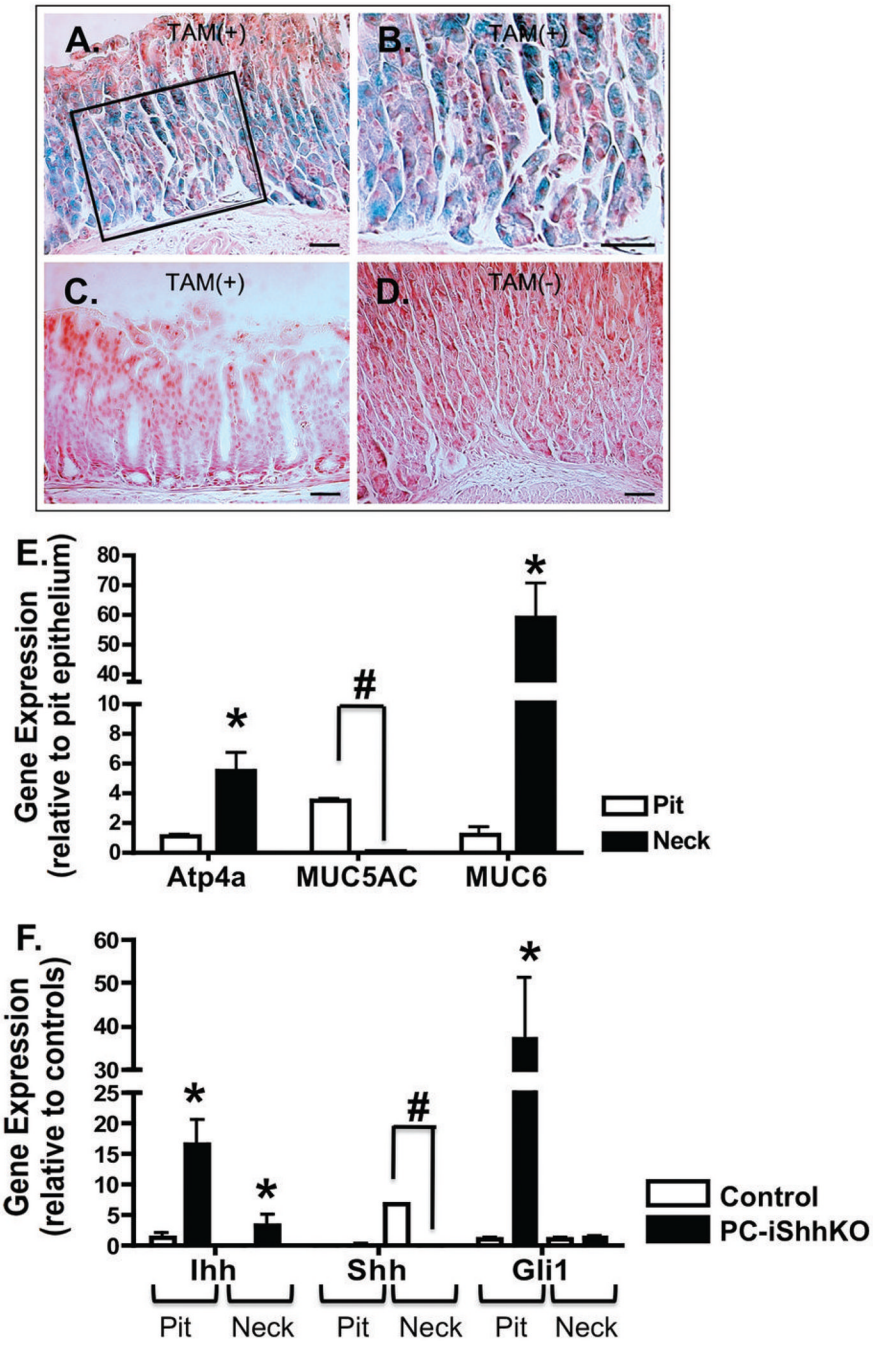

Figure 1. Verifying the successful generation of the mice expressing a parietal cell-specific deletion of Shh

(**A–D**) β-Galactosidase activity in the fundic mucosa of HKCre^{ERT2} mice crossed with Rosa26r^{lacZ} reporter mice. (**A**) Gastric fundic mucosa from representative HKCre^{ERT2}; Rosa26r^{lacZ} mouse treated with tamoxifen (TAM+) and processed for β-galactosidase activity staining with X-gal. (**B**) Shows highlighted area at higher power. X-gal staining blue parietal cells are present in the fundic mucosa. (**C**) No X-gal staining was observed in the antrum of a tamoxifen-treated HKCre^{ERT2};Rosa26r^{lacZ} mouse. (**D**) No X-gal staining was observed in the fundic mucosa of an HKCre^{ERT2}; Ro-sa26r^{lacZ} mouse that did not receive tamoxifen (TAM-). (**E,F**) Quantitative RT-PCR was performed on stomach RNA isolated

from gastric mucosa collected from control and PC-iShhKO mice. (**E**) Average fold change in gene expression of Atp4a (parietal cell marker), MUC5AC (pit cell marker) and MUC6 (neck cell marker) in RNA collected from the pit and neck regions of control mice. Data are presented as the mean ± SEM where $*P < 0.05$ significantly greater compared to pit region. #P<0.05 significantly lower compared to pit region, n = 4 mice/group. (**F**) Average fold change in gene expression of Ihh, Shh and Gli1 in RNA collected from the pit and neck regions of control and PC-iShhKO mice. Data are presented as the mean ± SEM where $*P < 0.05$ significantly greater compared to control group. #P<0.05 significantly lower compared to controls, n = 4 mice/group.

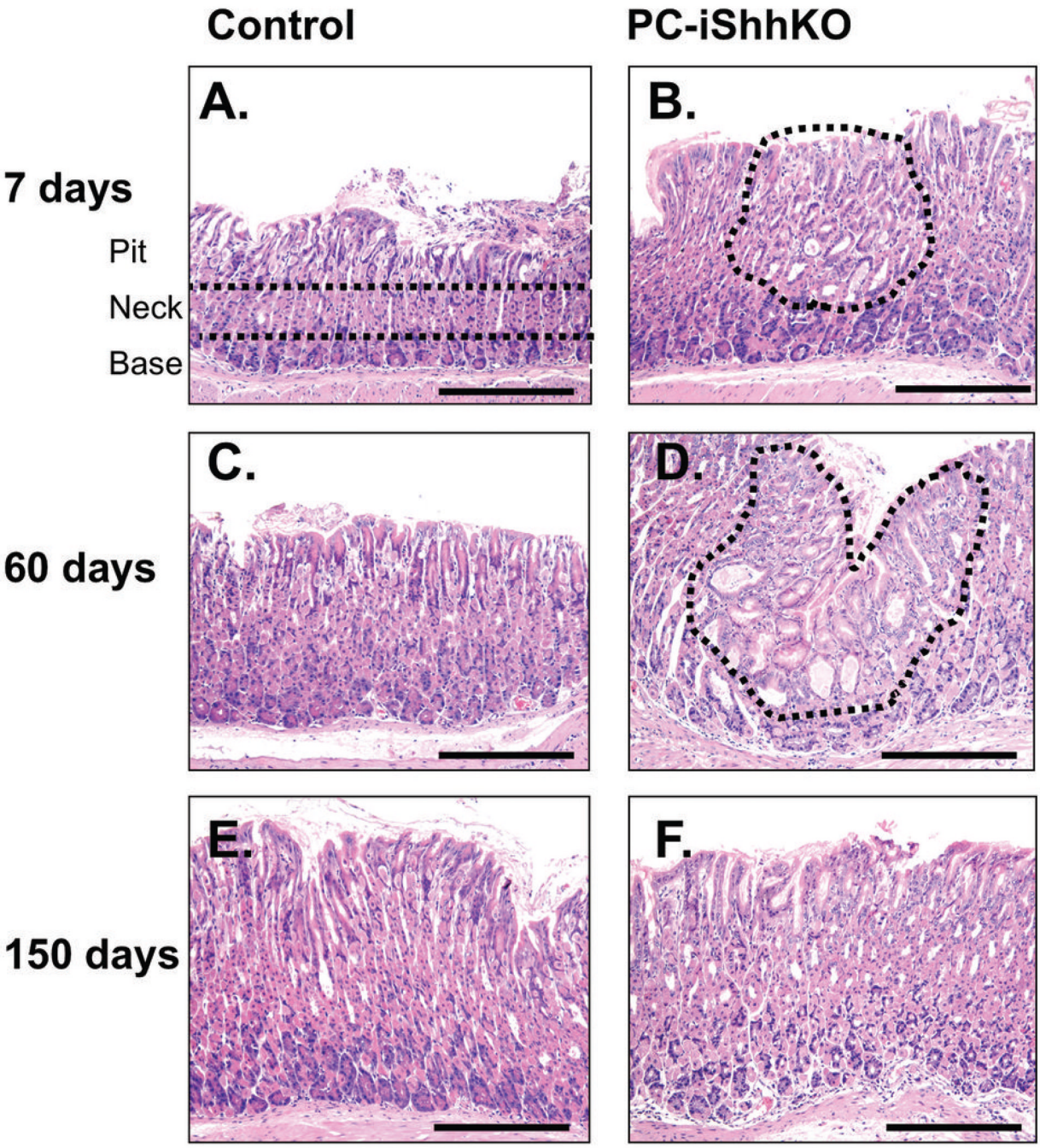

Figure 2. Histology of stomachs collected from control and PC-iShhKO mice

H&E staining of gastric tissue collected from (**A, C, E**) control or (**B, D, F**) PC-iShhKO mice 7, 30, 60 and 150 days after the final vehicle or tamoxifen injection. Representative images from n = 4–6 mice per group. Images were captured at 10X magnification. Scale bar = 150 microns.

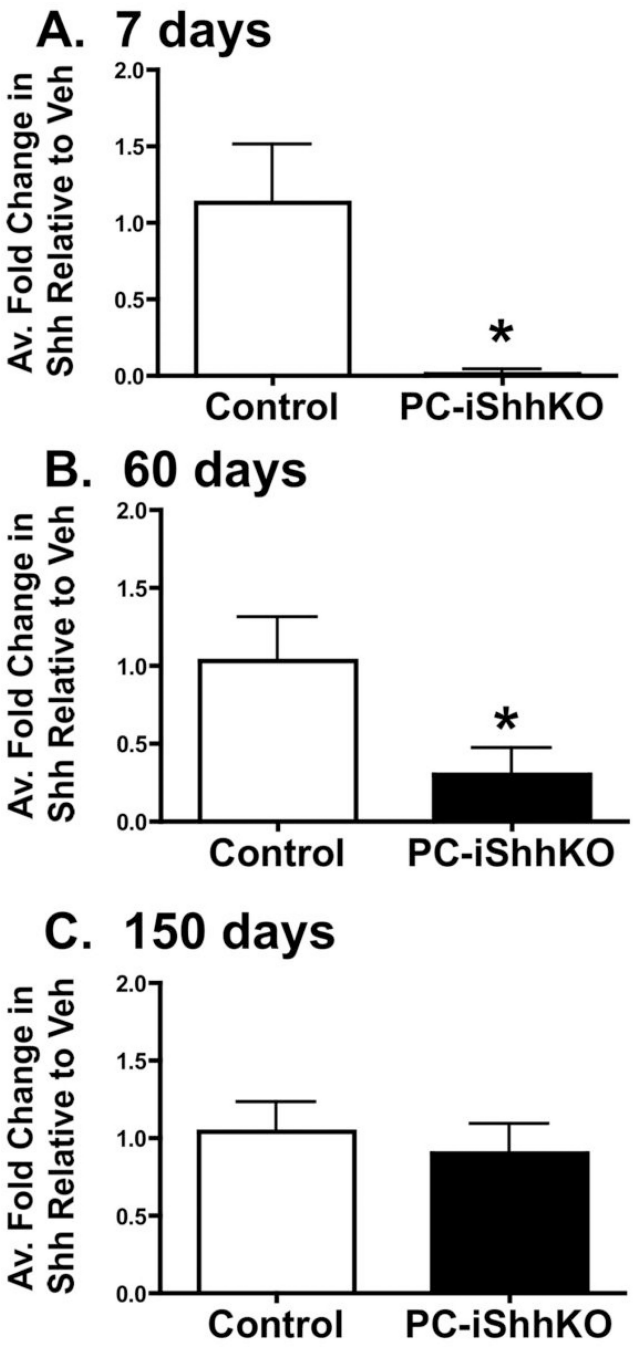

Figure 3. Re-expression of gastric Shh in control and PC-iShhKO mice

Quantitative RT-PCR was performed on stomach RNA isolated from gastric mucosa collected from control and PC-iShhKO mice. Shown is the average fold change in gene expression of Shh RNA collected from the neck region of control and PC-iShhKO mouse stomachs at (**A**) 7, (**B**) 60 and (**C**) 150 days after the final vehicle or tamoxifen injection. *P<0.05 compared to control group, n = 3–6 mice/group.

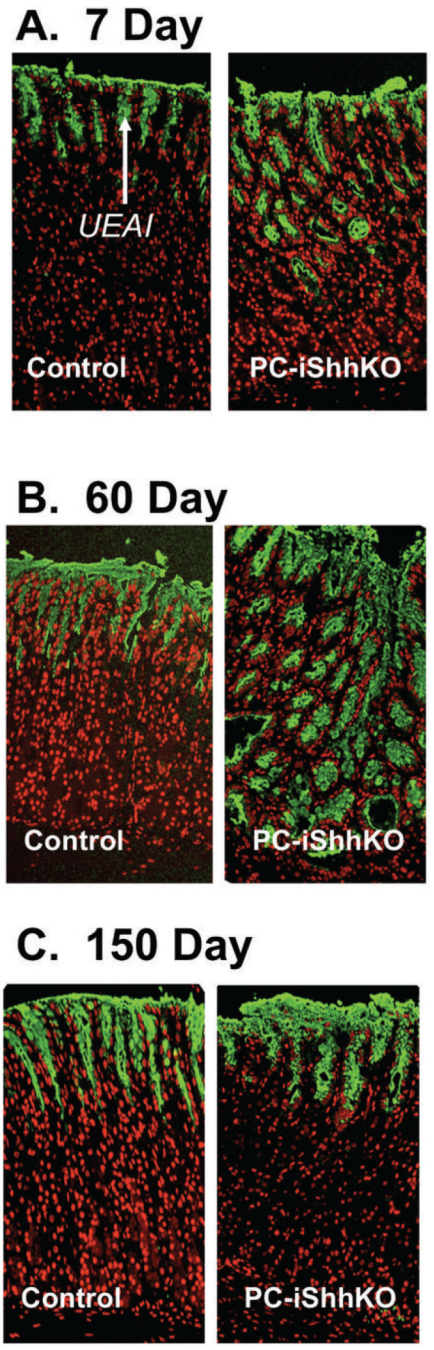

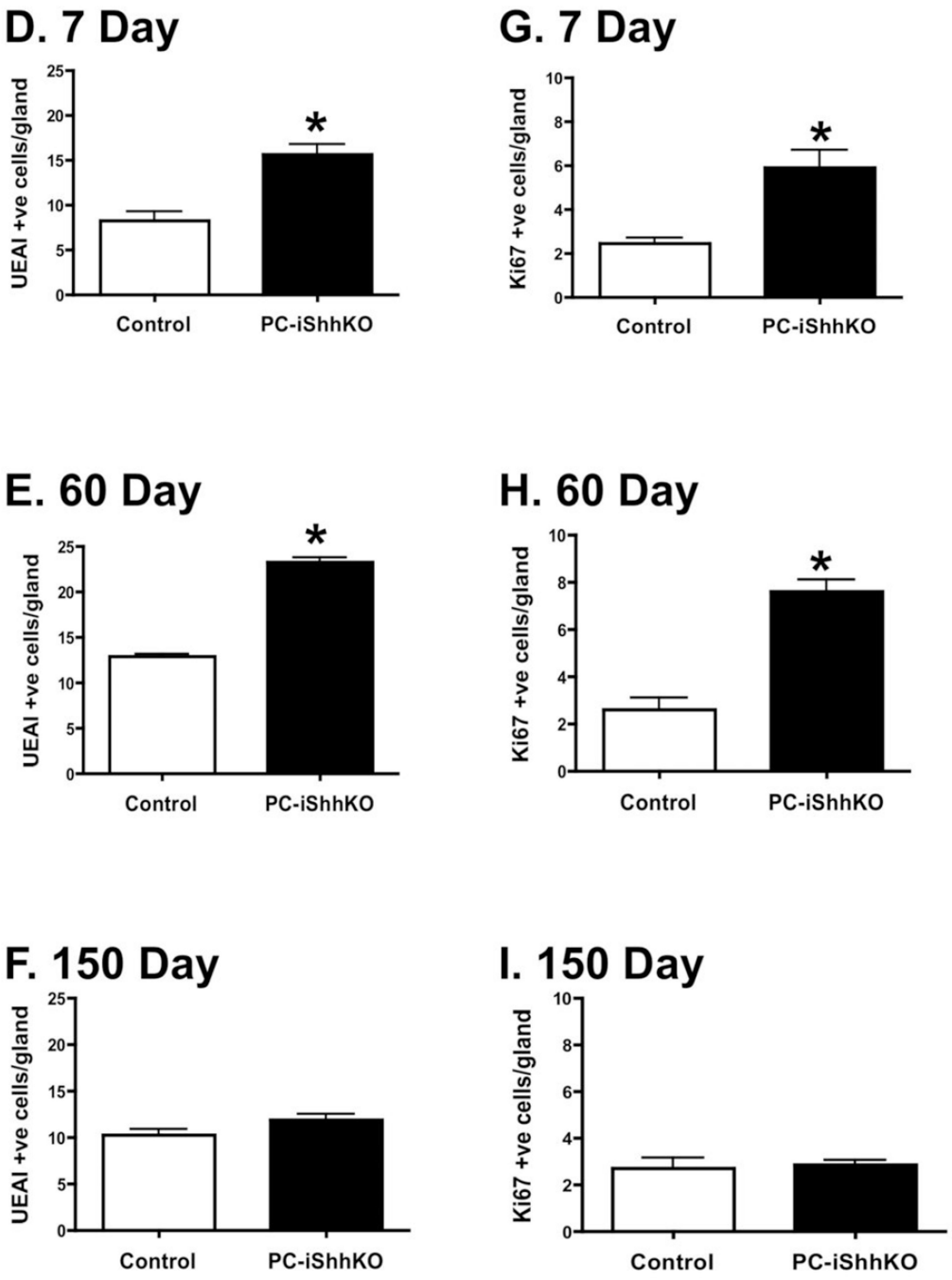

Figure 4. Expression of surface mucous pit and proliferating cells in control and PC-iShhKO mouse stomachs

Stomach sections collected from control and PC-iShhKO mice were immunostained for UEAI (surface mucous pit cells) (**A**) 7, (**B**) 60 and (**C**) 150 days after the final vehicle or tamoxifen injection. Morphometric analysis of UEAI +ve (surface mucous pit) cells/gland in control or PC-iShhKO mouse stomachs (**D**) 7, (**E**) 60 and (**F**) 150 days after the final vehicle or tamoxifen injection. Morphometric analysis of Ki67 +ve cells/gland in control and PC-iShhKO mouse stomachs (**G**) 7, (**H**) 60 and (**I**) 150 days after the final vehicle or tamoxifen injection. *P<0.05 compared to control group, n = 3–6 mice/group.

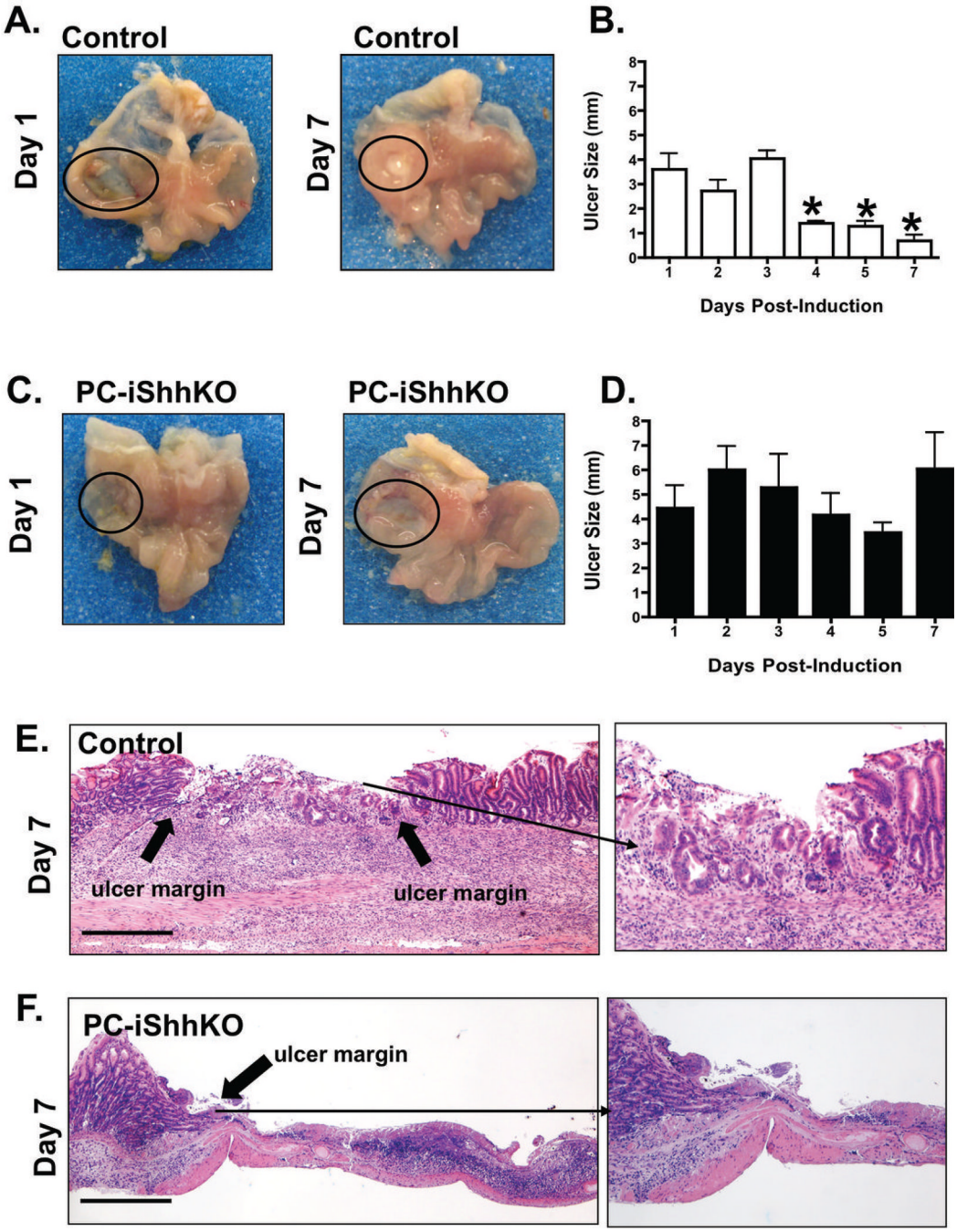

Figure 5. Wound healing in control and PC-iShhKO mouse stomachs

Gross morphology and ulcer sizes measured in mouse stomachs collected from (**A, B**) control and (**C, D**) PC-iShhKO mice 1 to 7 days after acetic acid-ulcer induction. Ulcers are circled on the figures **A** and **C**. Data is shown as mean + SEM of ulcer size (mm). *P<0.05 compared to control group, n = 6–8 mice/group. H&E staining of stomach sections collected from (**E**) control and (**F**) PC-iShhKO mice 7 days after acetic acid ulcer injury. Block arrows show the ulcer margin and inset is a higher magnification of the shown area. Images were captured at 4X magnification, images shown in inset were captured at 10X magnification. Scale bars = 375 microns.

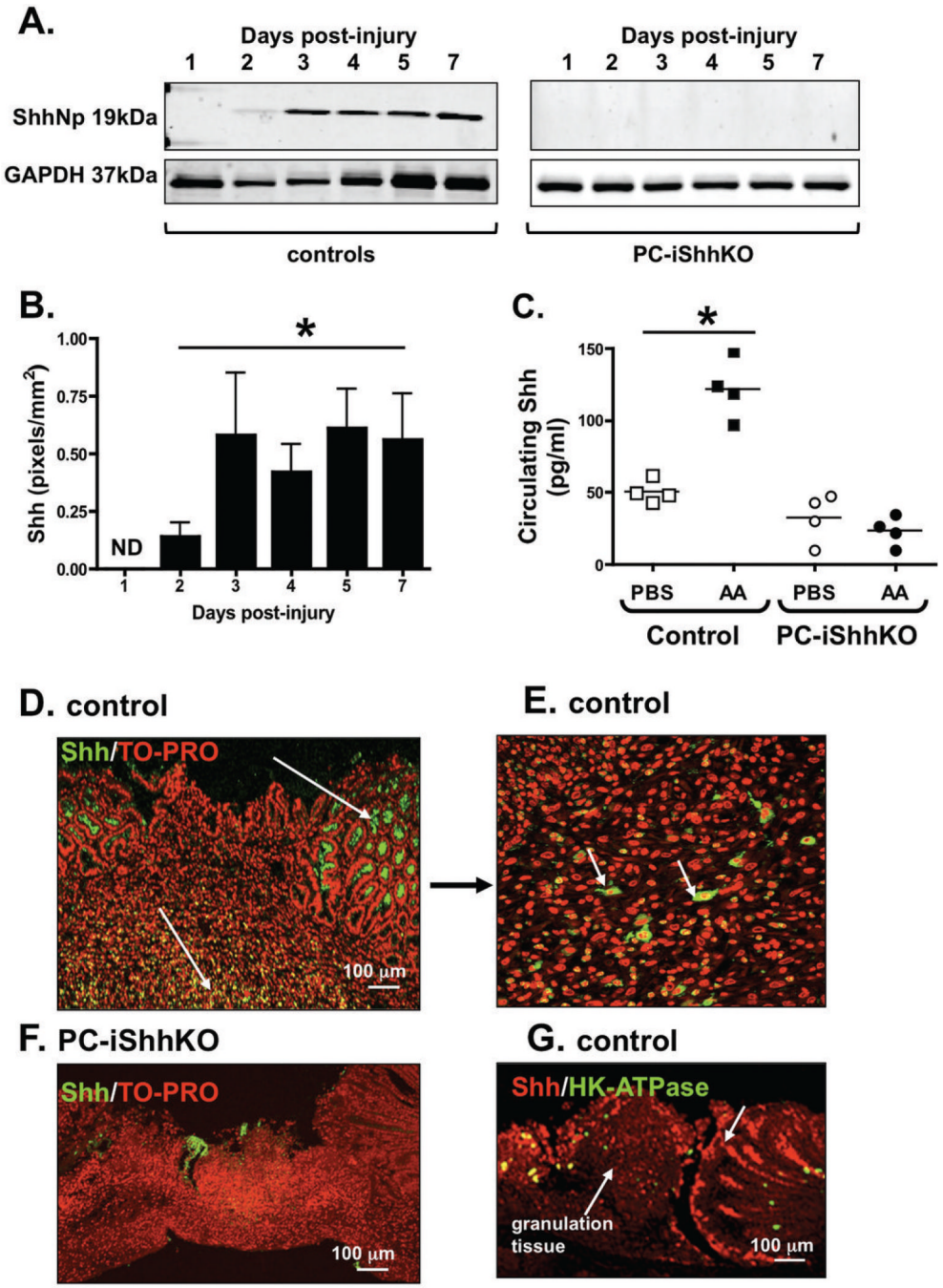

Figure 6. Shh protein expression in control and PC-iShhKO mouse stomachs during wound healing

(A) Representative western blot of ShhNp expression in a control and PC-iShhKO mouse stomach collected from the injured tissue at 1, 2, 3, 4, 5 and 7 days post-injury. **(B)** Quantification of Shh protein expression. Data are shown as means ± SEM for 3 individual experiments and expressed as Shh (pixels/mm^2), *$P < 0.05$ compared to day 1 injured tissue, ND: not detected. **(C)** Circulating Shh concentrations measured by ELISA using plasma collected from control and PC-iShhKO mice with PBS- (PBS) or acetic acid-induced (AA) injury 3 days post-surgery. *$P < 0.05$ compared to PBS controls. Im-munofluorescence staining using anti-Shh antibody of **(D, E)** control and **(F)** PC-iShhKO mouse stomachs 3

days post-induction of injury within the gastric mucosa. **(G)** Immunoflu-orescence staining of control mouse 3 days post-induction of injury within the gastric mu-cosa using antibodies specific for parietal cells (H+,K+-ATPase, green) and Shh (red).

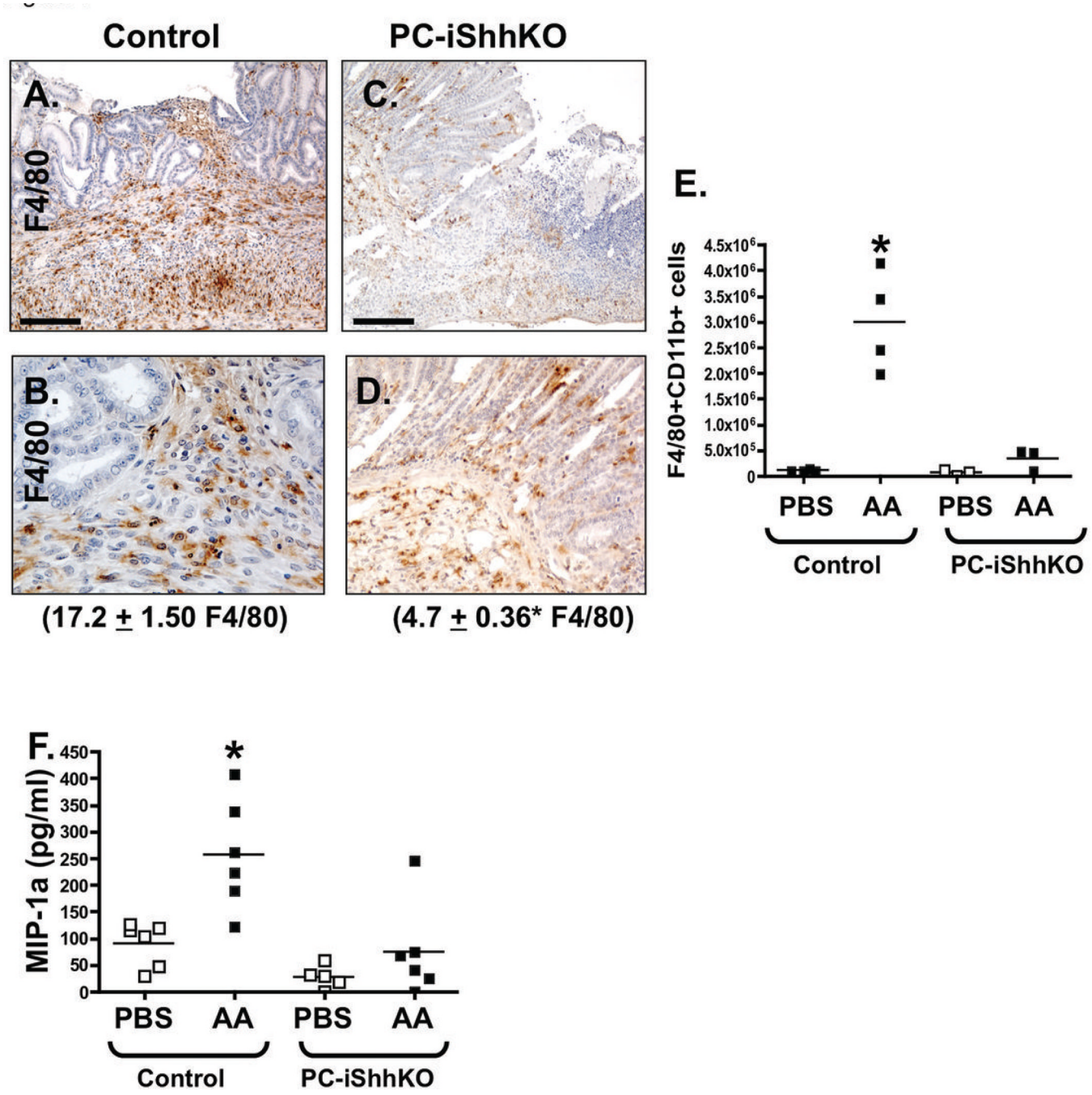

Figure 7. Macrophage infiltration at the ulcerated site in control and PC-iShhKO mice

Stomachs sections were collected from (**A, B**) control and (**C, D**) PC-iShhKO mice 2 days after ulcer induction and immunostained for myeloid cell marker F4/80. Representative figures of n = 6–8 mice per group. Images were captured at 20X magnification. Higher magnification images shown in **B** and **D** were captured at 40X magnification. Scale bars = 150 microns. The number of F4/80 positive cells were counted and expressed as the mean + SEM cells/high power field (shown in parentheses). *P<0.05 compared to controls, n = 6–8 mice/group. **(E)** Quantification of gastric $CD11b^{high}F4/80^{high}$ cells in control and PC-iShhKO mouse stomachs. (**F**) MIP-1α tissue concentrations measured in control and PC-iShhKO mouse stomachs. N = 5–6 mice per group, *P < 0.05 compared to PBS controls.

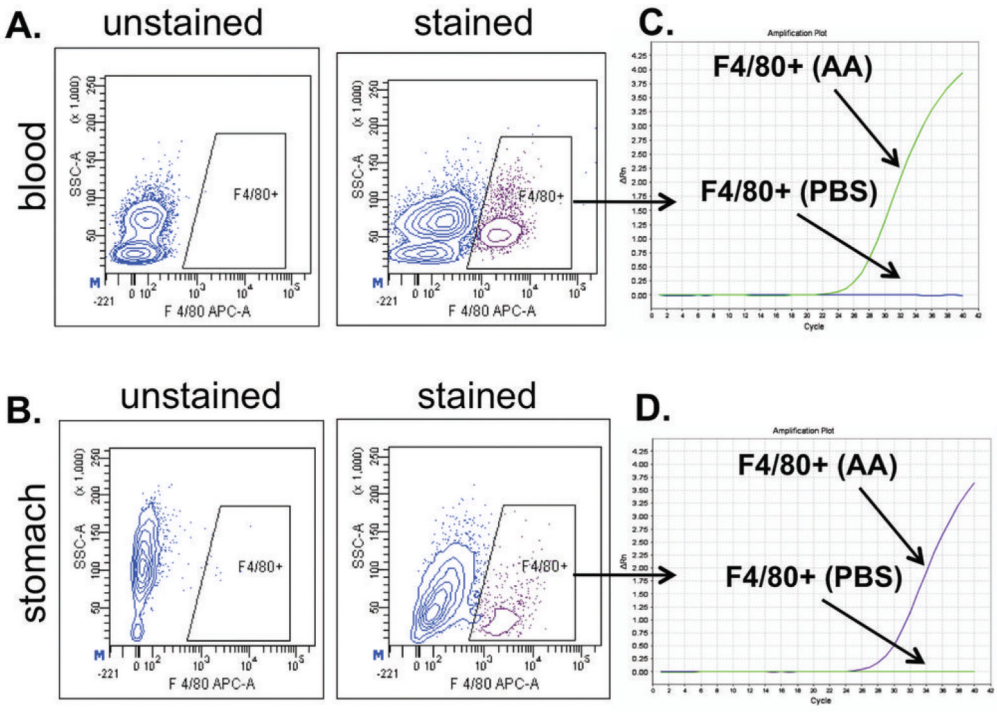

E.

BLOOD	Average Ct Value ± SEM	
	Gli1	Hhip
Controls		
PBS	ND	ND
AA	28.3 ± 0.41	23.3 ± 0.40
PC-iShhKO		
PBS	ND	ND
AA	ND	ND
STOMACH	**Average Ct Value ± SEM**	
	Gli1	**Hhip**
Controls		
PBS	ND	ND
AA	31.4 ± 0.56	26.2 ± 0.50
PC-iShhKO		
PBS	ND	ND
AA	ND	ND

ND: Not detected

Figure 8. Gli1 and Hhip expression in macrophages FASC sorted from peripheral blood and gastric tissue 3 days post-acetic acid-induced injury

Representative flow cytometric contour plots of the gating scheme for F4/80+ macrophages in **(A)** peripheral blood or **(B)** gastric tissue collected from control mice with acetic acid-induced injury 3 days post-surgery. The graphical representation of qRT-PCR data. Amplification plot of Rn (fluorescence of reporter dye divided by fluorescence of passive reference dye) plotted against the PCR cell cycle number in Gli 1 expression in FACS sorted macrophages from **(C)** peripheral blood and **(D)** gastric tissue collected from control mice. **(E)** Average Ct value in gene expression of Gli 1 and Hhip in RNA collected from FACS

sorted macro-phages from peripheral blood and gastric tissue from control and PC-iShhKO mice. ND: not detected.

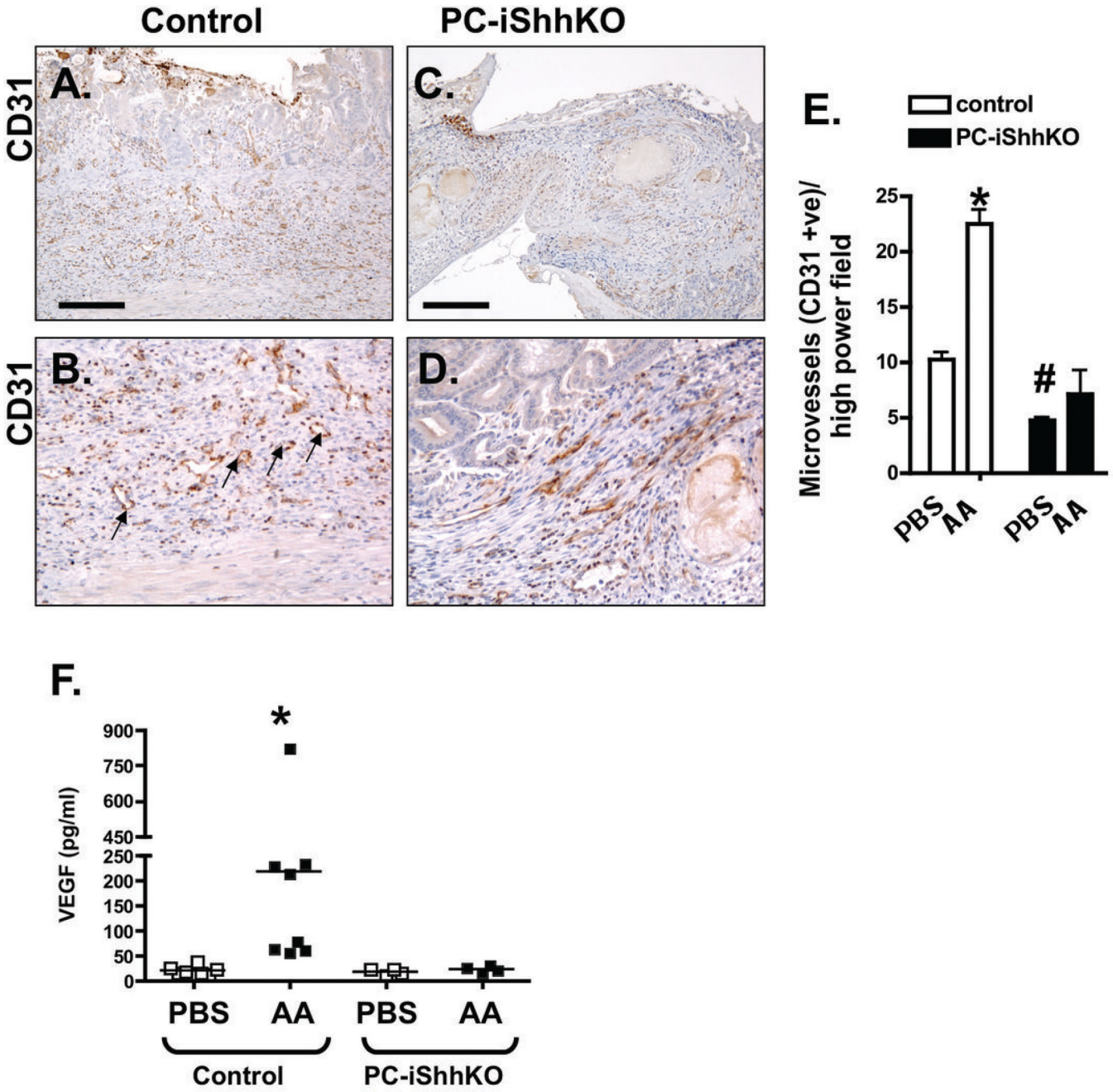

Figure 9. Expression of CD31 and VEGF in control and PC-iShhKO mouse stomachs during wound healing

Immunostaining for CD31 of stomach sections collected from (**A, B**) control and (**C, D**) PC-iShhKO mice 7 days after acetic acid ulcer induction. Images were captured at 20X magnification. Higher magnification images shown in **B** and **D** were captured at 40X magnification. Scale bars = 150 microns. Representative figures of n = 6–8 mice per group. (**E**) Microvessels were counted in PBS- and acetic acid (AA)-treated control and PC-iShhKO mice 7 days after induction of ulcers. Data is shown as mean + SEM. *P<0.05 compared to PBS-treated control, #P<0.05 compared to PBS-treated PC-iShhKO mice. n = 3–4 mice/group. (**F**) VEGF tissue concentrations measured in control and PC-iShhKO mouse stomachs. N = 5–6 mice per group, *P < 0.05 compared to PBS controls.